Available online at www.sciencedirect.com
ScienceDirect
Acta Materialia xxx (2008) xxx–xxx
Acta MATERIALIA
www.elsevier.com/locate/actamat

Bulk metallic glasses with large plasticity: Composition design from the structural perspective

Li Zhang [a], Yong-Qiang Cheng [b], A-Jing Cao [b], Jian Xu [a,*], Evan Ma [b,*]

[a] *Shenyang National Laboratory for Materials Science, Institute of Metal Research, Chinese Academy of Sciences, 72 Wenhua Road, Shenyang 110016, China*

[b] *Department of Materials Science and Engineering, The Johns Hopkins University, Baltimore, MD 21218, USA*

Received 12 August 2008; received in revised form 28 October 2008; accepted 1 November 2008

Abstract

While most bulk metallic glasses (BMGs) appear brittle at room temperature, appreciable compressive plastic strains have been observed for some glass compositions. The origin of this behavior is not understood, and the compositions of such plastic BMGs remain difficult to predict. Here we explain the plasticity observed in a Zr–Cu(Ni)–Al BMG, based on a computational analysis of the composition-dependent internal structures that influence shear transformations and shear localization behavior under loading. A strategy is then proposed to design BMG compositions with the desired local order for significant compressive plasticity, and is demonstrated by the successful discovery of an $Hf_{62}Ni_{25}Al_{13}$ BMG capable of sustaining large compressive strains. The experimentally measured compressive strength, glass transition temperature and Poisson's ratio, which are all composition dependent, are also shown to be macroscopic indicators that correlate well with the predictions from the atomic level structure.

Keywords: Amorphous materials; Metallic glasses; Mechanical properties; Plastic deformation; Structure

1. Introduction

Since the early 1990s, a large number of bulk metallic glasses (BMGs) have been discovered [1,2]. While the development of alloys with high glass-forming ability (GFA) continues to be important, recently more and more attention is being shifted towards the discovery of BMGs with a good combination of mechanical properties [1,3]. Of particular interest are the monolithic BMGs that possess not only the high strength known for glassy metals, but also large plasticity [3–9]. There have been several recent reports of "high/super ductility" [6,7] for BMGs [3–9]. Although these claims are actually not for uniform tensile elongation but for localized deformation in shear bands, the large compressive strains observed are nevertheless very interesting for fully glassy materials, and potentially useful for load-bearing applications.

So far large compressive plasticity has been found only at a handful of BMG compositions [4–9]. A number of factors have been invoked to explain the observations, including a high Poisson's ratio (ν) [4,10,11], nanocrystallization within shear bands [12–15], nanometer-scale heterogeneities [5], (spinodal) phase separation [9] in the glassy state, and excessive free volume content [8,16,17]. Most of these proposed mechanisms have not been well understood, and some are in fact quite controversial. Moreover, a particular challenge is that it has not been possible to predict a priori at what alloy compositions the BMGs would be plastic.

In this work, we approach the plasticity issue from a different perspective, and propose a microscopic explanation for the large plasticity observed, emphasizing the role of local order in the BMG atomic-level structure in influencing the shear transformations (STs) and shear banding

* Corresponding authors. Tel.: +86 24 23971950; fax: +86 24 23971215 (J. Xu); tel.: +1 410 516 8601; fax: +1 410 516 5293 (E. Ma).
E-mail addresses: jianxu@imr.ac.cn (J. Xu), ema@jhu.edu (E. Ma).

1359-6454/$34.00 © 2008 Acta Materialia Inc. Published by Elsevier Ltd. All rights reserved.
doi:10.1016/j.actamat.2008.11.002

behavior. The structural aspect will be examined using molecular dynamics (MD) simulations of realistic Zr–Cu–Al BMGs. The results offer insight into the high plasticity observed in related systems [7], as well as guidance for the experimental development of new BMGs with large plasticity. In particular, based on an understanding of how the internal structure changes with alloy composition, a strategy will be demonstrated to design BMG compositions that can sustain significant plastic strains. The usefulness of this strategy is then demonstrated by an example: the discovery of a plastic $Hf_{62}Ni_{25}Al_{13}$ BMG.

2. Materials and methods

Experiments were carried out in the Zr–Cu–Al and Hf–Ni–Al systems. Elemental pieces with purity >99.9 wt.% were used as starting materials. The master alloy Zr–Cu–Al and Hf–Ni–Al ingots with the nominal composition (in at.%) were prepared by arc melting under a Ti-gettered argon atmosphere in a water-cooled copper hearth. The master ingots were remelted several times to ensure compositional homogeneity, and then remelted in a mini-arc meter and suction-cast into a copper mold that has internal rod-shaped cavities about 35 mm in length.

The cross-sectional surfaces of the as-cast BMG rods were analyzed by X-ray diffraction (XRD) using a Rigaku D/max 2400 diffractometer with monochromated Cu K_α radiation. The glass transition and crystallization behavior of the as-cast samples were investigated using a Perkin-Elmer differential scanning calorimeter (DSC) under flowing purified argon with a heating rate of 0.33 K s^{-1}. The measured glass transition temperature, T_g, and the onset temperature of the first crystallization event, T_{x1}, were reproducible within ±2 K (at least three samples were measured for reproducibility).

Samples used for compression tests were 3 mm in height, cut from the cast rods of 1.5 mm in diameter. Uniaxial compression tests at room temperature were conducted on Shimadzu AG-1/500 KN universal testing machine using a constant strain rate of 1×10^{-4} s^{-1}. At least five samples were measured for each composition to ensure that the results are reproducible and statistically meaningful. The strain was determined from the platen displacement after correction for machine compliance.

The elastic constants of the BMGs were measured by resonant ultrasound spectroscopy (RUS). For each alloy, one machined cylindrical sample from the as-cast BMG rod of 2 mm in diameter was measured. The sample with known volume and mass was placed between the piezoelectric transducers. Two independent elastic constants C_{11} and C_{44} were obtained and used to calculate the elastic moduli, including shear modulus, bulk modulus and Poisson's ratio.

MD simulations were conducted for the Zr–Cu–Al ternary BMGs, employing embedded atom method (EAM) potentials. The samples, containing 10,000 atoms and with periodic boundary condition (PBC) applied for all three dimensions, were melted and equilibrated at 2000 K for 2 ns (time step 2 fs), and quenched into the glassy states (50 K) at a cooling rate of 100 K ns^{-1}. The temperature and pressure were controlled with a Nose–Hoover thermostat and a barostat, respectively. Geometrical analysis on the atomic configurations, using the Voronoi tessellation method, yields information about the atomic packing, such as the pair distribution functions (PDFs), atomic coordination numbers (CNs), types of coordination polyhedra, bond-angle distribution, etc. [18].

Pure shear loading of the 10,000-atom cubic box is conducted at 50 K, with PBC. The strain rate is 10^8 s^{-1}, and the box is deformed by supercell tilting followed by MD relaxation, with a step length of 2×10^{-7} in shear strain. Here the low temperature (50 K) was used to highlight the material responses upon mechanical activation, as the computer quenched glass structure after rapid cooling is usually more prone to thermal activation than real-world MGs that have experienced much more extended relaxation. At prescribed overall strains, we track the atomic strain of each atom, and dissociate the strain into the best affine fit and the minimum non-affine residue [19], thus capturing the ST event on atomic level. The ST is correlated with the atomic environment [18,19] given by its Voronoi coordination polyhedron.

Large-scale MD simulations of $Cu_{64}Zr_{36}$ and $Cu_{20}Zr_{80}$ MGs, prepared using the same cooling rate (1×10^{12} K s^{-1}), have been conducted to observe the initiation of shear bands. The samples were loaded in uniaxial tension at 50 K. The size of the two samples is $54.3 \times 27.2 \times 5.4$ nm^3, containing about 500,000 atoms each. A semicircular notch (9 nm in depth and 1 nm in notch radius) was introduced to facilitate shear band formation [20,21], simulating the inevitable stress concentrator in laboratory samples. PBC was applied for the Y- and Z-directions (see Fig. 5 below), while free surface was used for the X-direction. A constant strain rate (1×10^9 s^{-1}) along the Y-direction was used [16]. The plastic strain was examined by the atomic local strain tensor [22]: the reference configuration is the initial one prior to mechanical test.

3. Results

3.1. Structural explanation for the significant plasticity at certain Zr–Cu–Al BMG compositions

We start out by re-examining the previously reported "super-plastic" BMG [7], at the composition $Zr_{64}(Cu,Ni)_{26}Al_{10}$. In this case Liu et al. ruled out nanocrystallization or chemical inhomogeneity [7] as possible causes responsible for the large plasticity. To observe how such a BMG behaves differently from other compositions, we conducted compression tests of $Zr_{64}Cu_{26}Al_{10}$ (Z2) to compare with $Zr_{45}Cu_{45}Al_{10}$ (Z1). The reason for using ternary BMGs and not the original quaternary [7] is that we have interatomic potentials for computer simulations of the ternary (see below). As shown by the compression stress–

Please cite this article in press as: Zhang L et al., Bulk metallic glasses with large plasticity: Composition design from ..., Acta Mater (2008), doi:10.1016/j.actamat.2008.11.002

strain curve in Fig. 1a, the Z2 BMG can be plastically deformed to strains as large as ~7.5%. Beyond this point, the upper section of the sample contacted the bottom platen (see Fig. 2a), accompanied by sample tilt and subsequent cracking. The plastic strain beyond 7.5% is thus physically meaningless. Fig. 2a and b show the side-view appearance of the deformed Z2 sample after compression. As shown in Fig. 2b, a few shear bands roughly parallel to the major shear band are observed near the fracture surface. However, the plastic deformation is dominated by a single major shear band rather than pronounced multiple shear banding. The apparent plastic strain clearly originates from inhomogeneous shear deformation instead of homogeneous deformation. The test curve and scanning electron microscope features are all similar to what have been described in detail in Ref. [29]. In comparison, the curve for Z1 BMG exhibits practically no plastic strain (such compressive properties are consistent with previous

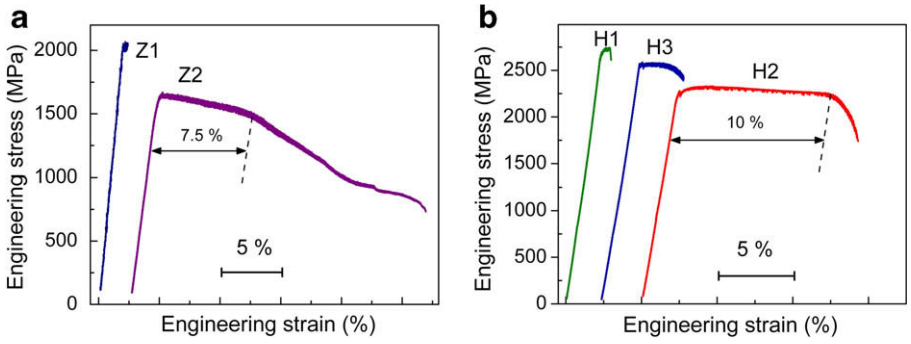

Fig. 1. Engineering stress–strain curves obtained from uniaxial compression tests of (a) $Zr_{45}Cu_{45}Al_{10}$ (Z1) and $Zr_{64}Cu_{26}Al_{10}$ (Z2), and (b) $Hf_{50}Ni_{25}Al_{25}$ (H1), $Hf_{55}Ni_{25}Al_{20}$ (H3) and $Hf_{62}Ni_{25}Al_{13}$ (H2). The curves are shifted relative to each other for clarity.

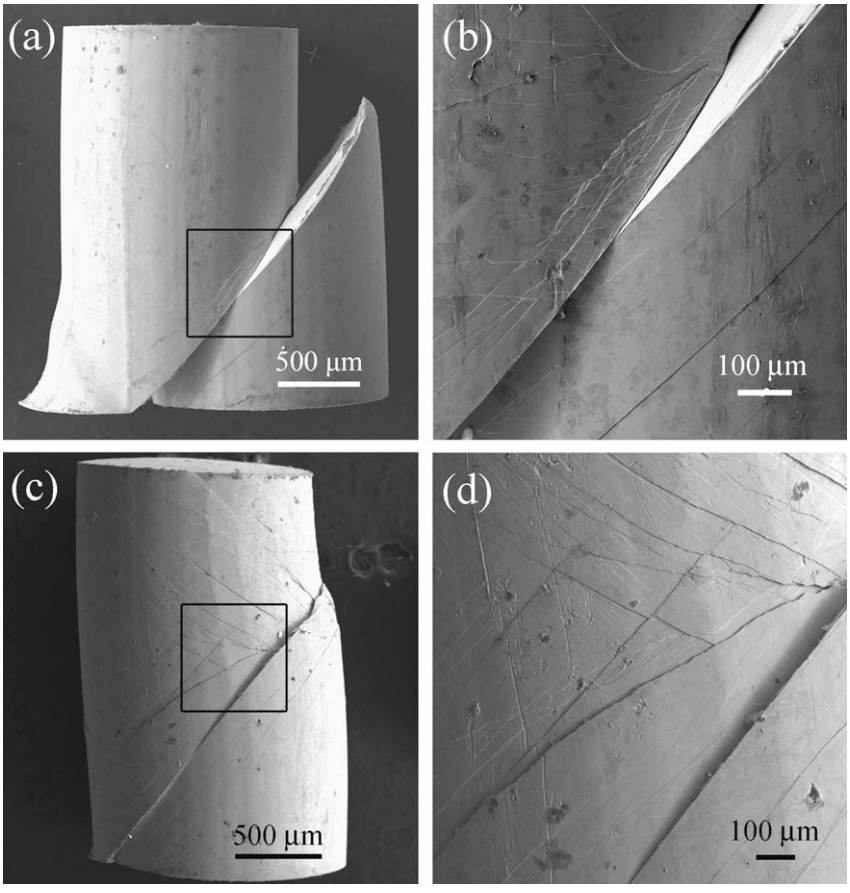

Fig. 2. Scanning electron micrographs (side view) for the BMG samples after compression: (a) Z2 and (c) H2; (b) and (d) are high-magnification images of the marked areas in (a) and (c), respectively.

Please cite this article in press as: Zhang L et al., Bulk metallic glasses with large plasticity: Composition design from ..., Acta Mater (2008), doi:10.1016/j.actamat.2008.11.002

work for the same BMG [15] and similar compositions such as $Zr_{48}Cu_{45}Al_7$ [23]). Clearly, there is a pronounced compositional dependence of the intrinsic plasticity of these fully glassy (monolithic) BMGs, for a given (ternary) system. An explanation to this observation will be presented in the rest of this section. Such an understanding will also offer an insight for devising a strategy to locate other plastic BMGs in the next section.

Mechanical properties of metallic materials are controlled by their structures at different length scales. For fully monolithic BMGs without the microstructure commonly seen in crystalline metals, it is natural to ask if the contrasting plastic behavior of the two BMGs in Fig. 1a is rooted in their internal atomic-level structure, i.e. the local order developed, and its compositional dependence. Our answer to this question is "yes", as illustrated via the following four steps.

As the first step, we affirm that differences in MG structure can indeed affect the propensity for configurational change under applied stresses, in particular the STs to yield plastic strains [24,25]. Using MD simulations employing the EAM potentials of the Zr–Cu–Al ternary BMGs [19], we have tracked the atomic strain of each atom during shear deformation, and dissociated the atomic strain into the best affine fit and the minimum non-affine residue [19,26]. The local ST event on an atomic level can then be recognized by a jump of the non-affine residue. After recording all the ST events, the propensity of each atom for ST under loading can be correlated with its local atomic environment as characterized by the Voronoi coordination polyhedron. As demonstrated in Ref. [19], there are some Cu atoms embedded in polyhedra that have either unfavorable CN, or unusually low symmetry (non-Kasper polyhedra) with Voronoi indices far away from those expected for the CN. These are the most uncomfortable and hence low-probability (low-population) local environments, which tend to be the more fertile sites for mediating STs. In contrast, the Cu atoms embedded inside the full icosahedra (Voronoi index $\langle 0,0,12,0\rangle$, CN = 12, with all nearest-neighbor pairs being 5-fold bonds) are the most unwilling to take part in plastic relaxation events.

This difference in propensity for STs can be intuitively understood: the CN = 12 full icosahedra, although not perfect due to the presence of multiple species with different sizes, have higher symmetry compared with other types of coordination, denser packing and higher configurational transition barrier, and are thus the most energetically favorable motifs and consequently the most reluctant to undergo ST events. In fact, a necessary condition for the onset of global plastic flow is for the applied stresses to disorder some of these relatively rigid full icosahedra, reducing their population to prepare the glass structure for flow (percolated STs) [19,27]. A similar controlling effect of full icosahedra on the thermally activated relaxation dynamics in supercooled liquid [28] offers additional proof that the full icosahedral packing is indeed the (rate-controlling) shear-resistant structural feature in the Cu–Zr-based MG system.

Based on this understanding achieved in our recent studies, one would expect that one route to improve plasticity is to reduce the resistance (or energy barrier) to flow initiation (this would be accompanied by some reduction in strength) and induce more flow regions and numerous ST events globally, so as to sustain more dispersed plastic strain before catastrophic failure. It follows from the discussion in the preceding paragraphs that the fraction of the ST-resistant icosahedral clusters should be minimized and the fraction of fertile regions maximized. Such a BMG structure, with more ready-to-flow regions, also decreases the chance for severe localization of plastic strains and energy/heat [19], allowing widened shear bands (see figures in Section 3.2 below, for evidence). The latter can also be a likely reason for the intermittent (stop-and-go) shear band propagation on the major shear plane observed for plastic BMGs [29] (such as that in Fig. 1a). In some cases, a large population of fertile sites is expected also to facilitate multiple shear band initiation and percolation, which is a frequent feature of plastic BMGs. In addition, the easier configurational adjustments may induce nanocrystallization in the later stages during shear deformation [12,15]. All these are helpful for observing large plastic strains before failure.

The second step is to show that there are indeed major structural differences, in terms of the populations of fertile/resistant sites for STs, between the two BMGs in Fig. 1a, such that the structural insight above could be relevant to their obvious difference in plasticity. A structural analysis on these two MGs using our MD-derived atomic configurations show that for the low-plasticity Z1 glass, the fraction of Cu-centered full icosahedra out of all types of polyhedra around Cu (f_{ico}^{Cu}) is 21%, while the fraction of full icosahedra out of all types of polyhedra around all atoms (Cu, Al and Zr, f_{ico}) is 14%. Since each icosahedraon contains 13 atoms, the fraction of atoms in the whole system that are involved in the full icosahedra (f_{ico}^{atoms}) is as high as 74%. In comparison, for the more plastic Z2 these numbers are much lower, at 7%, 5%, and 46%, respectively. A histogram showing these obvious structural differences is given in Fig. 3. These detailed structural data indeed support the view that structural motifs can be quite different

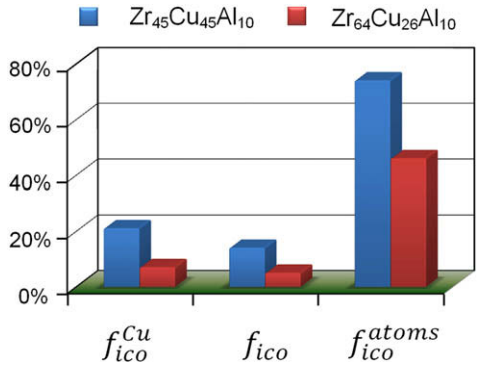

Fig. 3. Comparison of the degree of full icosahedal packing in $Zr_{45}Cu_{45}Al_{10}$ (Z1) and $Zr_{64}Cu_{26}Al_{10}$ (Z2).

Please cite this article in press as: Zhang L et al., Bulk metallic glasses with large plasticity: Composition design from ..., Acta Mater (2008), doi:10.1016/j.actamat.2008.11.002

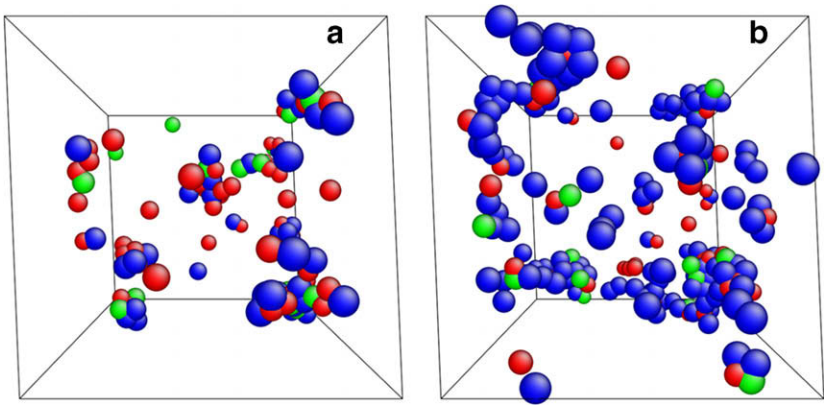

Fig. 4. Atoms that have participated in shear transformation events, after 5% shear strain: (a) $Zr_{45}Cu_{45}Al_{10}$; (b) $Zr_{64}Cu_{26}Al_{10}$. Color scheme: blue for Zr atoms, red for Cu atoms, green for Al atoms. (For interpretation of the references to color in this figure legend, the reader is referred to the web version of this article.)

at different compositions [19,30], and should thus play a critical role in the obviously different mechanical properties.

In the third step, we will directly demonstrate that the atomic-scale plastic behaviors of these two MGs are different in computer simulations. We first show that the number of atoms participating in ST events is different for Z1 and Z2. Fig. 4 shows that at 5% shear strain (before the global yield point [19] for the small MD sample, such that dispersed and isolated inelastic ST events can be observed), the number of atoms involved in STs for Z2 is ~70% larger than that for Z1. This implies a larger fraction of fertile sites to initiate STs in Z2, and a more homogeneous distribution of inelastic strain.

We next show that in larger-scale simulations, the shear localizations that subsequently initiate are also different (see Fig. 5a and b). For these relatively large-scale MD simulations, we use examples of binary Cu–Zr MGs to facilitate the analysis. We compare two compositions with very different solvent (Zr) content, to better reveal the differences in shear banding behavior. This choice is made, because due to the limited MD timescale (very fast quenching), the local ordering developed in the MGs (especially the Cu-rich one) would not be as much as in real-world BMG samples, and the structural difference for compositions that are not sufficiently far apart would not be sufficiently large, obscuring the structural effects on shear banding. Comparing Fig. 5a with b, at the same strain of 10%, the latter has more ST events (recorded with blue dots), obviously wider shear bands (less severe localization) and lower temperature (not shown) in the band. This result suggests that a lower icosahedra population encourages more ST events globally and could discourage catastrophic localization, and thereby promotes plasticity. The shear band in the Zr-rich BMG is clearly much wider, indicating less strain concentration, less chance of runaway instability, and therefore more likelihood for shear band arrest. Such a MG is expected to survive larger global plastic strain.

We note that our extensive simulations indicate that for Z1 the population of full icosahedra can increase markedly if the sample is treated with MD annealing (or slower cooling of the liquid), while for Z2, this effect is much weaker. Therefore, in the real-world BMG samples, the contrast between the two glasses (both structure and plastic behavior) should be more pronounced than in the simulation.

As the fourth step, we generalize the structural and deformation behavior found above for the two MGs. Based on a series of additional MD simulations to map out the compositional dependence in the Zr–Cu–Al system [19], the overall trend is that the fewer smaller (solute) Cu and Al atoms, the less the fraction of (Cu- or Al-centered) full icosahedra. This observation can be explained as follows (the principle is applicable also for the Hf–Ni–Al case below in Section 3.2). The Cu to Zr atomic size ratio is much smaller than the ideal size ratio of 0.902 for the formation of icosahedra, with Cu at the center, surrounded by Zr atoms only [18]. However, icosahedra will form more

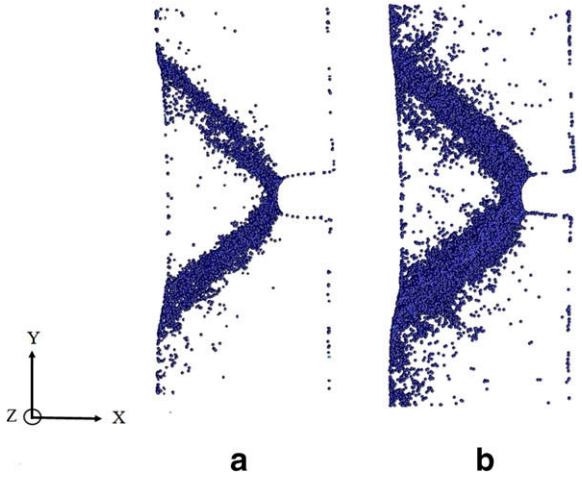

Fig. 5. Shear localization in two MGs of different compositions (both cooled at the same MD quench rate of 10^{12} K s^{-1}). In (a) for $Cu_{64}Zr_{36}$ MG, the fraction of icosahedra in Cu-centered polyhedra is about 19%, whereas that in (b) for $Cu_{20}Zr_{80}$ MG is 2%. For clarity, the atoms with local atomic strain smaller than a criterion value (0.35) are not shown.

Please cite this article in press as: Zhang L et al., Bulk metallic glasses with large plasticity: Composition design from ..., Acta Mater (2008), doi:10.1016/j.actamat.2008.11.002

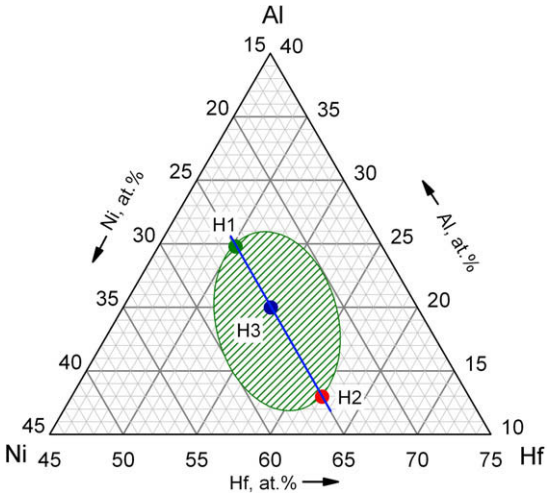

Fig. 6. Composition map for the formation of 3 mm diameter Hf-Ni-Al BMGs. The hatched region represents the BMG-forming zone. The compositions of the three BMGs discussed in text are marked as H1, H2 and H3.

easily when some Cu and Al atoms are mixed with Zr, in the first shell of Zr. This happens only when relatively high contents of Cu and Al are available. Since the size of Al is in between that of Zr and Cu, a number of combinations of the three species (Zr, Cu, Al) in the first shell of the central Cu can lead to an effective size ratio (center to first shell) close to the ideal ratio of 0.902 for icosahedral packing. The partially covalent-like character of the Al–metal bonding would also contribute to the stability of the icosahedral clusters. Some Al atoms themselves are also centers of full icosahedra. Therefore, to destabilize icosahedra formation, our alloy design should use concentrations of solutes (Cu and especially Al) that are as low as possible. In other words, the highest possible Zr content would be more desirable, from the plasticity standpoint, provided the GFA remains sufficient to make a bulk glass. In Ref. [7], Zr-rich $Zr_{64}(CuNi)_{26}Al_{10}$ turns out to be the best in terms of plasticity amongst the BMGs available in the Zr–(CuNi)–Al system.

3.2. Composition design for BMGs with large plasticity

Having explained the contrasting plastic behavior of the two Zr–Cu–Al ternary BMGs (Fig. 1a) from the structural perspective, the next challenge is to predict/design new BMGs with desired mechanical properties. In the following, we will illustrate our approach in several steps.

Our first step is to identify an alloy system that has a relatively wide composition range for BMG formation. This provides the composition space to tune the BMG composition for tailoring the structure and hence the strength/plasticity combination. The Hf–Ni–Al ternary system is one such case: our systematic studies have revealed a sizable composition zone (50–63 at.% Hf, 20–31 at.% Ni and 12–25 at.% Al) over which BMGs 3 mm in diameter can be formed via copper mold casting. This BMG-forming composition zone is the hatched region circled in Fig. 6. XRD patterns of three representative alloys are displayed in Fig. 7a, showing features typical of BMGs. Their calorimetry curves are displayed in Fig. 7b, showing clear glass transition and crystallization signals. Again, the relatively large BMG-forming zone offers the room to change the composition for optimized properties. This is a premise necessary for our approach: if an alloy system allows BMG formation only at a couple of compositions, the very limited composition choices would leave little opportunity for property design. Meanwhile, the wide BMG-forming zone also presents another challenge: a strategy is needed to guide us towards the BMG composition with the optimized properties. Our structural principle discussed above in Section 3.1 for Zr–Cu–Al ternary BMGs comes in handy for this purpose.

The second step is to conduct compression tests to acquire a sense of the plastic deformation behavior of the BMGs in the Hf–Ni–Al alloy system, to gauge if good plasticity is likely. In our Hf–Ni–Al case, compression tests of composition H1 ($Hf_{50}Ni_{25}Al_{25}$) on the low-Hf end in Fig. 6 indicate that Hf–Ni–Al BMGs do have the ability to sustain plastic deformation. A representative engineering stress–strain curve of composition H1 is displayed in

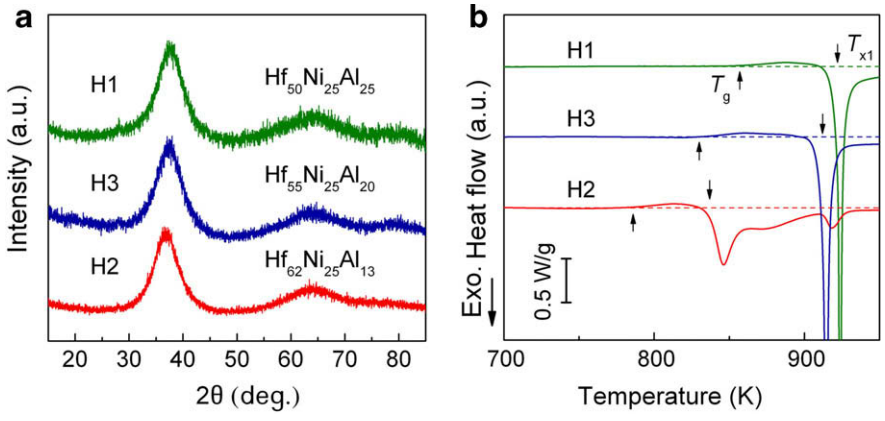

Fig. 7. (a) X-ray diffraction patterns of three Hf-based BMGs taken from the cross-sectional surface of the as-cast rods and (b) their differential scanning calorimetry curves.

Please cite this article in press as: Zhang L et al., Bulk metallic glasses with large plasticity: Composition design from ..., Acta Mater (2008), doi:10.1016/j.actamat.2008.11.002

Fig. 1b, showing yielding behavior and subsequent plastic strain. Although this BMG exhibits a plastic strain of only a couple of percentage this result is suggestive that at some other compositions it may be possible to achieve larger plastic strains. Conversely, if such tests indicate a completely brittle BMG, it would be uncertain if there exists any composition within the BMG-forming zone where the BMG can sustain plasticity. In other words, a starting point needs to be located at which the BMG has at least visible plastic deformability. We can then build on this initial BMG to optimize the composition and achieve better properties.

The third step, which is the key question this work addresses, is to decide on the direction one should go inside the BMG-forming zone in Fig. 6, to reach the highest plasticity possible. As mechanical properties can be strongly composition-dependent, a spread-out search would require small composition steps. With multiple samples at each composition for reproducibility and statistics, numerous alloys would have to be tested to map out the BMG-forming zone. This is undesirable, and clearly calls for a search strategy. To this end, we apply the structural design principle discussed above for the Zr–Cu–Al ternary BMGs.

The question then becomes: in the fairly wide Hf–Ni–Al BMG-forming zone in Fig. 6, how does the glass structure change with composition, and in which direction should we go starting from H1 to minimize the icosahedra population and maximize the population of fertile regions? As discussed earlier for the Zr–Cu–Al system, the answer is that we should move towards lower concentrations of the solutes (now Ni and Al), i.e. higher solvent (Hf) concentration. In the BMG-forming zone in Fig. 6, H2 ($Hf_{62}Ni_{25}Al_{13}$) would be the composition where this is maximized.

To observe the difference in the internal glass structure, for H2 vs. H1, we again make use of our Zr–Cu–Al EAM potentials for simulations of $Zr_{50}Cu_{25}Al_{25}$ and $Zr_{62}Cu_{25}Al_{13}$, to mimic H1 and H2, respectively, (potentials are not available for the Hf–Ni–Al ternary). This is of course an approximation just to confirm the trend, but its relevance can be justified as follows. In terms of tabulated atomic sizes, Zr (radius $r_{Zr} = 0.158$ nm) and Hf ($r_{Hf} = 0.167$ nm), and Cu ($r_{Cu} = 0.127$ nm) and Ni ($r_{Ni} = 0.128$ nm), are close. In terms of chemical properties, Zr and Hf are in the same column of the periodic table, while Cu and Ni are next-door neighboring late transition metals. In order to check the similarity in electronic structure, we also compared the ab initio MD simulation results from both systems (for this purpose a small box with ~100 atoms was used), as shown in Fig. 8. The charge density distribution and atomic configuration are quite similar. Charge density distribution at the sites of Al (green) in contact with Cu or Ni (gold) tends to be localized, suggesting some covalent-like character away from the hard-sphere like nature. This may reduce plasticity, in addition to the full icosahedral packing. Therefore, while some Al is necessary for the GFA, the Al content should be kept at a relatively low level to help preserve plasticity [15], by holding down not only the population of the Al-centered full icosahedra, but also the covalent-like bonding. Here by some degree of "covalent-like" character we refer to the polarized charge density distribution localizing between Cu and Al. It should be noted that the atoms at Al sites still appear to be close packed, indicating that the angular dependence, if any, is not strong. This justifies our use of the EAM potential.

The results for these two specific compositions are in line with the expectation from the general trend mentioned

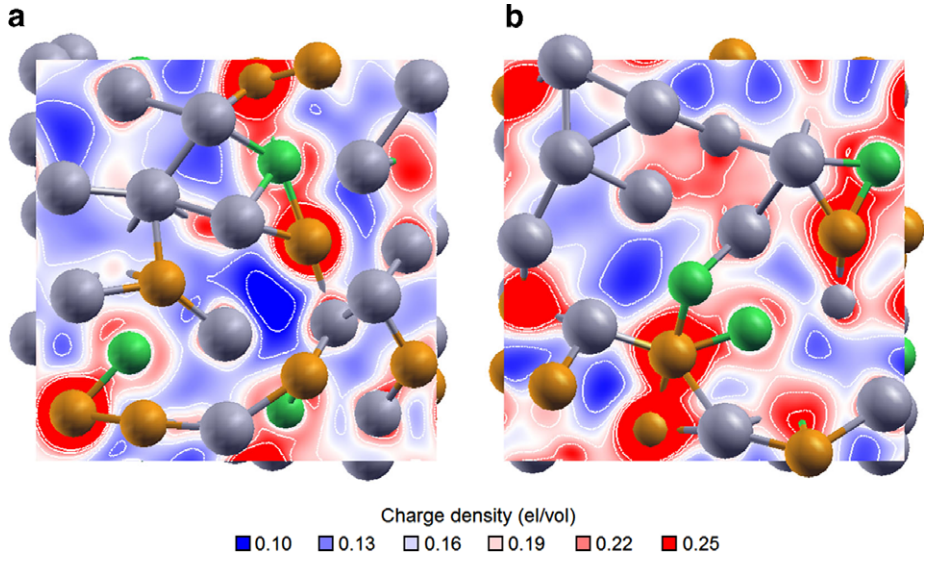

Fig. 8. Ab initio MD simulations of charge density distribution of (a) $Zr_{62}Cu_{25}Al_{13}$ and (b) $Hf_{62}Ni_{25}Al_{13}$, showing the similarity in electronic structure between these two MG systems. The grey balls represent Zr or Hf. Charge density distribution at the sites of Al (green) in contact with Cu or Ni (gold) tends to be localized. (For interpretation of the references to color in this figure legend, the reader is referred to the web version of this article.)

Please cite this article in press as: Zhang L et al., Bulk metallic glasses with large plasticity: Composition design from ..., Acta Mater (2008), doi:10.1016/j.actamat.2008.11.002

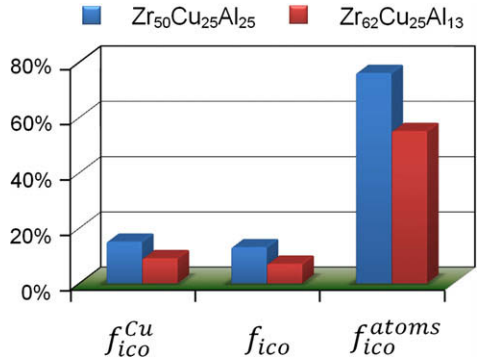

Fig. 9. Comparison of full icosahedal packing in $Zr_{50}Cu_{25}Al_{25}$ (to mimic $Hf_{50}Ni_{25}Al_{25}$) and $Zr_{62}Cu_{25}Al_{13}$ (to mimic $Hf_{62}Ni_{25}Al_{13}$).

above for previous simulations of the Zr–Cu–Al BMGs. For the more solute-rich $Zr_{50}Cu_{25}Al_{25}$, the fraction of full icosahedra around Cu is 15%, the total fraction of full icosahedra around all atoms is 13%, and the fraction of atoms involved in full icosahedra is 76%. In contrast, all these values indeed drop to much lower levels for the solvent-rich $Zr_{62}Cu_{25}Al_{13}$, at 9%, 7%, and 55%, respectively. A comparison showing these obvious differences is given in the histogram in Fig. 9. The trend for $Hf_{50}Ni_{25}Al_{25}$ and $Hf_{62}Ni_{25}Al_{13}$ would presumably be similar.

We then predict that moving from the low-Hf end (H1) to the highest-Hf end (H2, $Hf_{62}Ni_{25}Al_{13}$) of the BMG-forming zone, the STs should become easier and more numerous, as explained in Ref. [19]. In addition, the trend seen in Fig. 5 suggests the possibility of forming wider and less catastrophic shear bands as the solvent content increases. These should result in increased plasticity and reduced strength. A stress–strain curve (representative of the eight tests we conducted; see Table 1 for the spread of properties) for H2, is compared with H1 in Fig. 1b. As predicted, the strength is reduced relative to H1, but the plastic strain is much larger. In fact, H2 may be considered to have "large" compressive plasticity, for two reasons. First, the magnitude of the plastic strain reaching 10% is much larger than those of H1 and other brittle BMGs [3], and we observe multiple shear bands in the scanning electron microscopy observations (shown in Fig. 2c and d). Second, even after the large shear displacement of the major shear band sheared off part of the sample to touch the platen in a compression test, most of the tested samples did not break apart, similar to the "super-plastic" BMG [7,29] and the Z2 BMG in Fig. 2a. Note that further testing to continue the stress–strain curve is meaningless because the multiple contacts with the platen causes the true contact area to increase and may lead to an inflection point on the stress–strain curve, after which the load (and nominal engineering stress) rises drastically [29,31] (this is the behavior of several previous BMGs claimed to be "super-ductile" [6] or "super-plastic" [7]). In any case, our structural and compositional design has resulted in another BMG with significant plasticity (Fig. 1b).

The structural characteristics are also reflected by, and can correlate with, other properties such as the compressive strength and glass transition temperature T_g. These properties are composition dependent and are in fact useful macroscopic indicators. The T_g and compressive properties including yield strength and plastic strain of the Zr–Cu–Al and Hf–Ni–Al ternary BMGs are listed in Table 1. The lower content of icosahedral order in the BMG at Z2 and H2 is consistent with their lower T_g [28], which is known to scale with the yield strength, as has also been demonstrated previously for many BMGs [1,28,32]. A BMG composition with lower icosahedral ordering, and hence lower resistance to plastic flow, would exhibit a lower T_g, as discussed in our recent work [28]. In the absence of structural information shown in Figs. 3 and 9, one can then use T_g as an indicator of the internal structure, to gauge the direction to move the BMG composition for optimized mechanical properties. For the $Hf_xNi_{25}Al_{75-x}$ ($50 \leqslant x \leqslant 62$) BMGs (Table 1), T_g decreases linearly with increasing Hf content, at a rate of about 6.6 K at.%$^{-1}$, as shown in Fig. 10a. Another composition H3 ($Hf_{55}Ni_{25}Al_{20}$, also marked in Fig. 6), whose Hf content is in between those of the H1 and H2, has a T_g value between those of H1 and H2. The strength and plasticity values indeed fall in the middle as well, as shown in Fig. 1b and Table 1. This trend suggests that one can look for compositions with lower T_g (with accompanying reduced strength [28]) to achieve larger plasticity.

The shear modulus (G) and Poisson's ratio (ν) are other useful empirical indicators of the underlying, more fundamental structure–property relationship. The ν values of the BMGs discussed here, together with their G and bulk modulus (B), are also included in Table 1 and plotted in Fig. 10. As can be seen from Table 1, in our given alloy

Table 1
Glass transition temperature, elastic constants and compressive properties of the ternary Zr–Cu–Al and Hf–Ni–Al BMGs.

Alloys	Composition (at.%)	T_g (K)	G (GPa)	B (GPa)	ν	σ_y (MPa)	ε_p (%)
Z1	$Zr_{45}Cu_{45}Al_{10}$	708	35.4	113.3	0.359	2040–2050	0–0.5
Z2	$Zr_{64}Cu_{26}Al_{10}$	662	28.7	104.0	0.373	1660–1710	6–7.5
H1	$Hf_{50}Ni_{25}Al_{25}$	857	47.0	127.8	0.336	2720–2730	0.5–2
–	$Hf_{53}Ni_{25}Al_{22}$	838	43.3	125.3	0.345	–	–
H3	$Hf_{55}Ni_{25}Al_{20}$	828	43.7	127.2	0.346	2560–2570	2–3
–	$Hf_{58}Ni_{25}Al_{17}$	801	41.3	125.5	0.351	–	–
–	$Hf_{60}Ni_{25}Al_{15}$	791	40.8	122.8	0.350	–	–
H2	$Hf_{62}Ni_{25}Al_{13}$	779	41.3	128.8	0.355	2260–2320	5–10

Please cite this article in press as: Zhang L et al., Bulk metallic glasses with large plasticity: Composition design from ..., Acta Mater (2008), doi:10.1016/j.actamat.2008.11.002

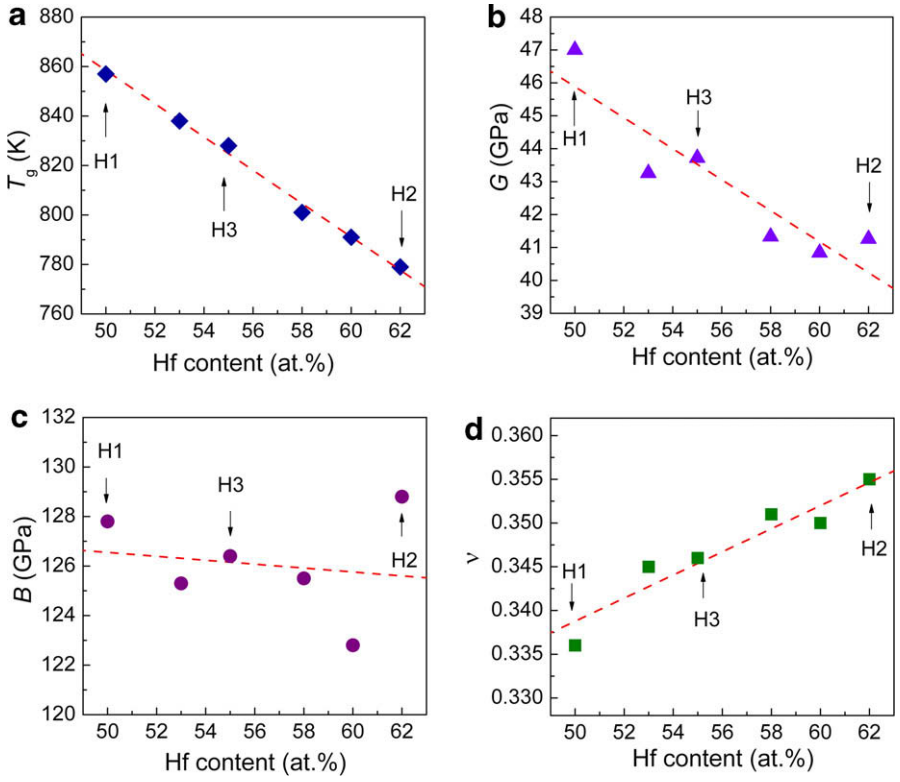

Fig. 10. Glass transition temperature T_g, shear modulus G, bulk modulus B and Poisson's ratio v, as a function of Hf content for the ternary $Hf_xNi_{25}Al_{75-x}$ BMGs.

system, the variation of the G or v is consistent with the predicted change in mechanical properties. In contrast to the alloy Z1, the alloy Z2 has a much lower G and higher v, and exhibits a lower σ_y and larger ε_p. The same trend is also true for the $Hf_xNi_{25}Al_{75-x}$ ($50 \leqslant x \leqslant 62$) BMG series. As shown in Table 1 and Fig. 10b–d, with increasing Hf content, the G value drops by about 0.5 GPa at.%$^{-1}$, whereas the B values are not significantly changed (around 125 ± 3 GPa), leading to a nearly linear increase in v from 0.336 at H1 to 0.355 at H2. A glass structure more resistant to shear (and hence reduced propensity for plastic events) is seen to have a higher G/B ratio or lower v. Conversely, BMGs with lower G and higher v, due to reduced icosahedral population in the internal structure, are more prone to STs which mediate plasticity. In other words, our structural design for high plasticity is consistent with the general idea of moving towards compositions with lower G/B ratio or higher v [1,3,4,10].

4. Discussion

The role of local structure in BMGs, particularly the non-dense local region (such as free volume), in affecting plasticity has been discussed by a number of authors (e.g. [16,17,27,30]). In our discussions here, however, we are not simply using the vague idea of different contents of free volume, but have emphasized a quantitative comparison of different degrees of local order for different compositions. We believe that free volume (or packing density) alone is not a sufficiently telling parameter: the difference between the free volume content in a ductile glass and a brittle glass is subtle and difficult to measure. Also, the free volume can be viewed as a by-product of structural disorder, as discussed in Ref. [33].

We point out that the local order we evaluated, e.g. the number of atoms involved in icosahedra, is meant to show the differences between BMGs at different compositions, but cannot be used to quantitatively predict the plastic strain achievable in compression tests. There is no quantitative criterion to predict the plastic strain of BMGs, based on the fraction of full icosahedra. Our goal here is to provide a new insight into the structure–property relationship of MGs, by a comparison of two trends: the changing plasticity observed experimentally, and the changed ordering in simulation.

Quantitative correspondence between simulations and experiments is not appropriate for a number of reasons. To begin with, the complete process of plastic deformation in experiment, from individual ST events to localized shear banding to eventual sample failure, is complicated and not well understood [1,3]. Our work only looks at the influence of the internal structure on the early stages of deformation, in particular the intrinsic propensity of the glass structure to sustain plastic flow. This propensity is relevant to the plasticity mechanisms, from individual ST events to localized shear banding to eventual sample failure, and may be reflected by the measured compressive plastic strain (although not necessarily in a quantitative way). In other

Please cite this article in press as: Zhang L et al., Bulk metallic glasses with large plasticity: Composition design from ..., Acta Mater (2008), doi:10.1016/j.actamat.2008.11.002

words, we are using the obviously different plastic strains of the glasses to illustrate that these different glass structures do intrinsically behave differently in their plasticity (other factors such as nanocrystals [15] and loading confinement [23,29,31] are not included).

It is certainly well known that nanocrystallization during shear banding can significantly affect the plasticity of MGs [12,14,15]. To be sure about this effect, one needs to examine the shear bands inside the tested samples carefully. This is not a trivial task. Shear bands are scarce and difficult to observe even when found; transmission electron microscopy (TEM) samples have to be prepared with great care to avoid artifacts [12,15]. We have not yet acquired such TEM information for our samples. However, if it turns out that there is indeed different tendency for nanocrystallization in the alloys we studied here, this tendency may also be dependent on the initial glass structure. A more rigid local structure with lower energy, such as the full icosahedra, may be less prone to nanocrystallization and hence exhibit lower plasticity. In fact, it has been reported that when Al was added into a Cu–Zr glass exceeds a certain level, nanocrystallization in shear bands ceases to occur and the BMG becomes more brittle [15]. This trend is consistent with the structure–property correlation discussed above (less Al is desirable for better plasticity). Therefore, the composition-dependent structure remains a valid perspective for the design of BMGs with improved plasticity.

Another issue requiring discussion is the spatiotemporal limitation of MD simulations. MD simulations are indeed different from the real process, in terms of both sample preparation and deformation. One should not therefore focus on the exact numbers, but on the trend and composition dependence. Our "design" is not quantitative in terms of comparing a composition with a pre-determined gauge, but is meant to hint at a direction to follow in the composition map in order to optimize the desired properties. The glass structure we produced in computer simulations cannot reproduce exactly the same configuration as in the real BMGs. Therefore the fraction of full icosahedra is only used as a measure to allow the simulated modes to reveal the structural trend. However, our findings do show convincing evidence for a consistent trend of the compositional dependence of the atomic structure and the intrinsic mechanical properties. The measured plastic strain can be considered as a qualitative measure of the latter, and the simulated degree of local order (and composition dependence) is a qualitative indicator of the former. A theoretical and quantitative linkage between the two is difficult to come by, but we believe the trend and correlation should be valid and enlightening, as also demonstrated in our previous work [19,28].

BMGs have been obtained in many different alloy systems. Our discussion here focuses on Cu–Zr-based BMGs. For other types of BMGs, for example those based on transition metal-metalloid systems, the dominant order and property-controlling polyhedra may be of other types, and the nature of bonding (e.g. the higher degree of covalent bonding in those systems) could be of higher importance [18,34]. The composition design for large plasticity may therefore require additional structural and chemistry considerations and is a subject for future study.

5. Summary

Most BMGs exhibit very small plastic strains in uniaxial compression tests at room temperature, bordering on brittle behavior. A handful of glass compositions, however, have been reported previously to be able to sustain relatively large compressive plastic strains. We have added another example here: Hf-based BMGs (see Fig. 1b). We feel that even for monolithic, uniformly amorphous BMGs, their plasticity can still be markedly different, due to the strong composition dependence of the degree of short-range order developed in the internal structure of the BMGs. This explanation for large variations in plasticity is based on our analysis of the composition-dependent internal structures (Figs. 3 and 9). We believe that the high Zr content, which discourages the development of full icosahedral local order that strongly influences shear transformations and shear banding behavior under loading (Figs. 4 and 5), is a likely reason for the significant plasticity observed in $Zr_{64}(CuNi)_{26}Al_{10}$ [7] and $Zr_{64}Cu_{26}Al_{10}$ (Fig. 1a) BMGs.

A structural design strategy is then proposed to predict BMG compositions with appreciable compressive plasticity. By going for the most structurally favorable composition in the BMG-forming composition zone, we have discovered an $Hf_{62}Ni_{25}Al_{13}$ BMG capable of sustaining large compressive strains (Fig. 1b), demonstrating the usefulness of our strategy and the significance of understanding the structural origins.

While the microscopic understanding of the role of structure (in the case of monolithic BMGs, structure at the nanometer and subnanometer scale) is important for predicting properties, in some cases the structural information is difficult to come by. One can use macroscopic indicators, however, to gauge the property trends resulting from the changes in composition (and internal structure). Our structural insight indicates that the compressive strength (Fig. 1), G/B ratio and T_g would all go down when the glass structure is tuned to favor plasticity. As shown in Table 1 and Fig. 10, these macroscopic indicators, including ν which inversely correlates with G/B, are all in line with our structural predictions and hence have their common origin in the structural order. A combination of the atomic-scale understanding with the empirical correlations should greatly elevate our capability for designing BMGs with high plasticity.

Acknowledgments

The authors thank Prof. H.W. Sheng for the EAM potentials he developed while he was at The Johns Hopkins University. The authors gratefully acknowledge stimulating discussion with Prof. Y. Li and Prof. T.G. Nieh. This

work is supported at SYNL by National Basic Research Program of China (973 Program) under Contract No. 2007CB613906, and at The Johns Hopkins University by the US Department of Energy, BES-DMSE, under Contract No. DE-FG02-03ER46056.

References

[1] Greer AL, Ma E. MRS Bull 2007;32:611.
[2] Li Y, Poon SJ, Shiflet GJ, Xu J, Kim DH, Löffler JF. MRS Bull 2007;32:624.
[3] Yavari AR, Lewandowski JJ, Eckert J. MRS Bull 2007;32:635.
[4] Schroers J, Johnson WL. Phys Rev Lett 2004;93:255506.
[5] Das J, Tang MB, Kim KB, Theissmann R, Baier F, Wang WH, et al. Phys Rev Lett 2005;94:205501.
[6] Yao KF, Ruan F, Yang YQ, Chen N. Appl Phys Lett 2006;88:122106.
[7] Liu YH, Wang G, Wang RJ, Zhao DQ, Pan MX, Wang WH. Science 2007;315:1385.
[8] Chen LY, Fu ZD, Zhang GQ, Hao XP, Jiang QK, Wang XD, et al. Phys Rev Lett 2008;100:075501.
[9] Du XH, Huang JC, Hsieh KC, Lai YH, Chen HM, Jang JSC, et al. Appl Phys Lett 2007;91:131901.
[10] Lewandowski JJ, Wang WH, Greer AL. Philos Mag Lett 2005;85:77.
[11] Poon SJ, Zhu AW, Shiflet GJ. Appl Phys Lett 2008;92:261902.
[12] Chen MW. Annu Rev Mater Res 2008;38:060407.
[13] Saida J, Deny A, Setyawan H, Kato H, Inoue A. Appl Phys Lett 2005;87:151907.
[14] Lee SW, Huh MY, Chae SW, Lee JC. Scripta Mater 2006;54:1439.
[15] Kumar G, Ohkubo T, Mukai T, Hono K. Scripta Mater 2007;57:173.
[16] Li QK, Li M. Appl Phys Lett 2006;88:241903.
[17] Murali P, Ramamurty U. Acta Mater 2005;53:1467.
[18] Sheng HW, Luo WK, Alamgir FM, Bai JM, Ma E. Nature 2006;439:419.
[19] Cheng YQ, Cao AJ, Sheng HW, Ma E. Acta Mater 2008;56:5263.
[20] Bailey NP, Schiøtz J, Jacobsen KW. Phys Rev B 2006;73:064108.
[21] Cao AJ, Wei YG. Phys Rev B 2007;76:024113.
[22] Shimizu F, Ogata S, Li J. Mater Trans 2007;48:2923.
[23] Wu WF, Li Y, Schuh CA. Philos Mag 2008;88:71.
[24] Schall P, Weitz DA, Spaepen F. Science 2008;318:1895.
[25] Argon AS, Demkowicz MJ. Metall Mater Trans A 2008;39A:1762.
[26] Falk ML, Langer JS. Phys Rev E 1998;57:7192.
[27] Lee SC, Lee CM, Lee JC, Kim HJ, Shibutani Y, Fleury E, et al. Appl Phys Lett 2008;92:151905.
[28] Cheng YQ, Sheng HW, Ma E. Phys Rev B 2008;78:014207.
[29] Song SX, Bei H, Wadsworth J, Nieh TG. Intermetallics 2008;16:813.
[30] Park K, Jang J, Wakeda M, Shibutani Y, Lee JC. Scripta Mater 2007;57:805.
[31] Mondal K, Kumar G, Ohkubo T, Oishi K, Mukai T, Hoho K. Philos Mag Lett 2007;87:625.
[32] Yang B, Liu CT, Nieh TG. Appl Phys Lett 2006;88:221911.
[33] Cheng YQ, Ma E. Appl Phys Lett 2008;93:051910.
[34] Gu XJ, Poon SJ, Shiflet GJ, Widom M. Acta Mater 2008;56:88.

Please cite this article in press as: Zhang L et al., Bulk metallic glasses with large plasticity: Composition design from ..., Acta Mater (2008), doi:10.1016/j.actamat.2008.11.002